Geomechanics and Engineering, *Vol. 33, No. 5 (2023) 463-475*
https://doi.org/10.12989/gae.2023.33.5.463

Analysis of pile group behaviour to adjacent tunnelling considering ground reinforcement conditions with assessment of stability of superstructures

Young-Jin Jeon[1a] and Cheol-Ju Lee*[2]

[1]*College Institute of Industrial Technology, Kangwon National University, 1 Kangwondaehak-gil, Chuncheon-si, Gangwon-do, Republic of Korea*
[2]*Department of Civil Engineering, Kangwon National University, 1 Kangwondaehak-gil, Chuncheon-si, Gangwon-do, Republic of Korea*

(*Received October 10, 2022, Revised March 13, 2023, Accepted March 26, 2023*)

Abstract. Tunnel construction activity, conducted mainly in mountains and within urban centres, causes soil settlement, thus requiring the relevant management of slopes and structures as well as evaluations of risk and stability. Accordingly, in this study we performed a three-dimensional finite element analysis to examine the behaviour of piles and pile cap stability when a tunnel passes near the bottom of the foundation of a pile group connected by a pile cap. We examined the results via numerical analysis considering different conditions for reinforcement of the ground between the tunnel and the pile foundation. The numerical analysis assessed the angular distortion of the pile cap, pile settlement, axial force, shear stress, relative displacement, and volume loss due to tunnel excavation, and pile cap stability was evaluated based on Son and Cording's evaluation criterion for damage to adjacent structures. The pile located closest to the tunnel under the condition of no ground reinforcement exhibited pile head settlement approximately 70% greater than that of the pile located farthest from the tunnel under the condition of greatest ground reinforcement. Additionally, pile head settlement was greatest when the largest volume loss occurred, being approximately 18% greater than pile head settlement under the condition having the smallest volume loss. This paper closely examines the main factors influencing the behaviour of a pile group connected by a pile cap for three ground reinforcement conditions and presents an evaluation of pile cap stability.

Keywords: ground reinforcement; pile group; stability evaluation; three-dimensional numerical analysis; tunnel construction

1. Introduction

Currently, tunnel construction activity is conducted mainly in urban areas and mountains to provide convenient and safe infrastructure; this activity causes the deformation of the ground and hence serviceability of adjacent structures maybe of great importance. For tunnels constructed in mountainous areas, especially near a tunnel portal, and cloud-based platforms need to be developed for risk assessments using various smart sensors. In particular, the tunnel construction activity in urban centres often occurs adjacent to various existing structures, leading to soil settlement that affects the engineering aspects of the behaviour of piles (Lee 2012a). Studies have reported that tunnel construction activity near an existing pile foundation results in soil settlement, causing shear stress transfer between the piles and adjacent soil; this, in turn, leads to the deformation of the piles and alters the axial force distribution (Lee 2012a, b). To address these problems, researchers have conducted numerous investigations using indoor model experiments, centrifugal model experiments, theoretical studies, and numerical analysis (Jacobsz 2002, Pang 2006, Cheng *et al.* 2007, Lee and Chiang 2007, Lee 2008, Marshall 2009, Lee 2012a, b, c, Ng *et al.* 2013, Dias and Bezuijen 2014a, b, Hartono *et al.* 2014, Liu *et al.* 2014, Ng and Lu 2014, Ng *et al.* 2014, Williamson 2014, Hong *et al.* 2015, Jeon and Lee 2015, Jeon *et al.* 2015, Lee and Jeon 2015, Lee *et al.* 2016, Jeon *et al.* 2017, Jeon *et al.* 2018, Soomro *et al.* 2018, Jeon *et al.* 2020a, b, Ayasrah *et al.* 2020, Ayasrah *et al.* 2021, Qiu *et al.* 2022). However, studies involving field measurements and their analyses remain relatively limited. Selemetas (2005), Pang (2006), Liu *et al.* (2014), Mair and Williamson (2014), Williamson (2014), and Selemetas and Standing (2017) investigated the behaviour of piles adjacent to tunnel construction activity using field measurements. Most prior studies simply analysed only the behaviour of piles as affected by tunnel construction; significantly limited research has been devoted toward evaluating the stability of and damage to the pile cap and superstructure connected to piles. Fig. 1 shows the criterion of Son and Cording (2005) for evaluating damage to adjacent structures caused by ground movement due to tunnel construction and ground excavation activity, according to the lateral strain (ε_L) and angular distortion (β) in two dimensions. Son and Cording (2005) also proposed an evaluation criterion for the damage to adjacent structures based on the damage evaluation criterion presented by Boscardin and Cording (1989), for which they modified and supplemented the simplified

*Corresponding author, Professor
E-mail: cj32@kangwon.ac.kr
[a]Senior Researcher

ISSN: 2005-307X (Print), 2092-6219 (Online)

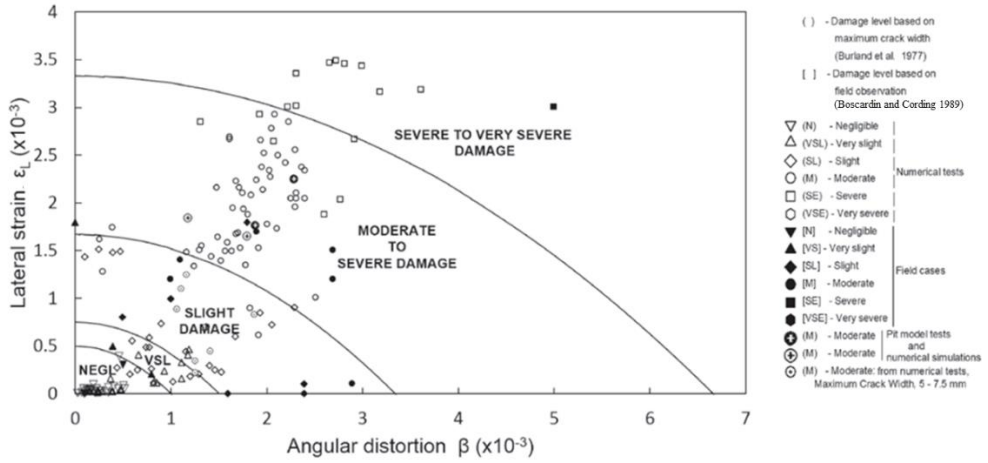

Fig. 1 Structure damage evaluation criterion based on angular distortion (β) and lateral strain (ε_L) (Son and Cording 2005)

assumptions for the problem of predicting structure damage. Son and Cording (2005) classified structural damage according to the lateral strain (ε_L) value for each section: (1) negligible, (2) very slight, (3) slight, (4) moderate to severe, or (5) severe to very severe.

Selemetas (2005) reported that the pile settlement caused by tunnel excavation considerably exceeds the pile settlement caused by application of the design load to the piles prior to tunnel excavation, and that the distribution of axial force acting on the piles during tunnel excavation is very sensitive to depth. Tunnel construction activity in urban centres causes soil settlement and requires that stability be secured for various structures above and below ground. However, there is insufficient systematic research into the effective prevention of the degradation of their stability and usability. Pile and pile cap settlement caused by tunnel-excavation-induced soil settlement is the factor that most greatly reduces the stability of the superstructure. Although a variety of reinforcement methods are applied in the field to solve this problem (Choi *et al.* 2005, Jue and Na 2005), the behavioural mechanisms and stability of structures according to tunnel construction have not been clearly identified. Therefore, systematic research that incorporates the existing stability evaluation criteria and considers a variety of reinforcement conditions for ensuring the stability of structures is needed.

Accordingly, in this study, we conducted a three-dimensional (3D) finite element analysis (FEA) to examine the effects on pile behaviour and pile cap stability of three reinforcement conditions for the ground around a tunnel during tunnel excavation under a 4 × 3 pile group connected by a pile cap. Thus, we analysed tunnelling-induced pile settlement, axial force, relative displacement, and shear stress and performed a stability evaluation.

2. Numerical analysis

2.1 Analysis overview and boundary conditions

In this study, we simulated tunnel construction activity performed beneath a 4 × 3 pile group connected by a pile cap in order to analyse pile behaviour according to the grouting reinforcement conditions in the soil adjacent to the tunnel. The simulation was performed using Plaxis 3D (2020), a 3D FEA program. Fig. 2(a) shows a representative finite element mesh used in the analysis, and Figs. 2(b) and 2(c) show cross sections of the analysis geometry. The mesh sizes used in the model considered the element distribution to coarse mesh. The diameter (D) of the tunnel used in the numerical analysis was 8 m, and the springline of the tunnel was located 26.5 m below the surface of the soil. The entire ground was assumed to be the weathered soil layer, for which general material properties in South Korea were assumed; the details are given in Section 2.2. As most prior studies focused mainly on small-diameter piles, for this study, we chose to use large-diameter cast-in-place piles with an assumed diameter (d) of 1 m. The axial force, shear stress, and relative displacement calculated in the study were based on the part of the pile embedded in the ground, whose length (L_p) was 20 m. The spacing between centres of the piles in the pile group was assumed to be 3d. We analysed the pile behaviour during tunnel excavation according to three conditions for grouting reinforcement in the ground around the tunnel. The thickness of the grout body was varied as 1 m or 2 m with the reinforcement angle fixed at 180°, and the reinforcement length for one reinforcement was 4 m; details of the reinforcement

Table 1 Summary of numerical analyses

Analysis series	Ground reinforcement angle	Ground reinforcement thickness (T)	Description
PLT	–	–	Pile load test
Gr	–	–	Greenfield
P	–	–	Pile group without ground reinforcement
RP1	180°	1 m	Pile group with 1 m ground reinforcement
RP2	180°	2 m	Pile group with 2 m ground reinforcement

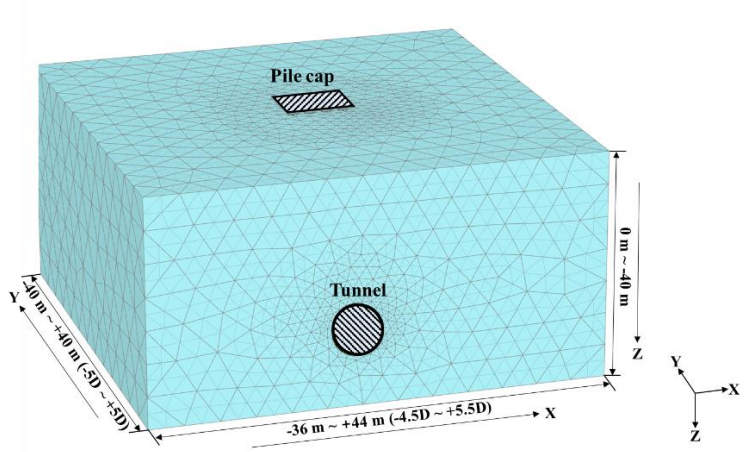

(a) Representative 3D finite element mesh used in the study (4 × 3 pile group) (*D*: tunnel diameter)

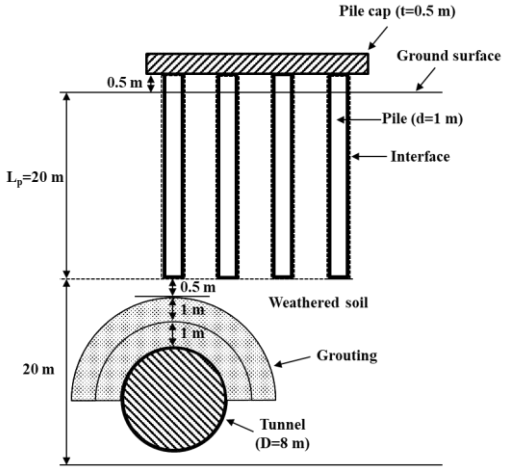

(b) Sectional view of analysis geometry

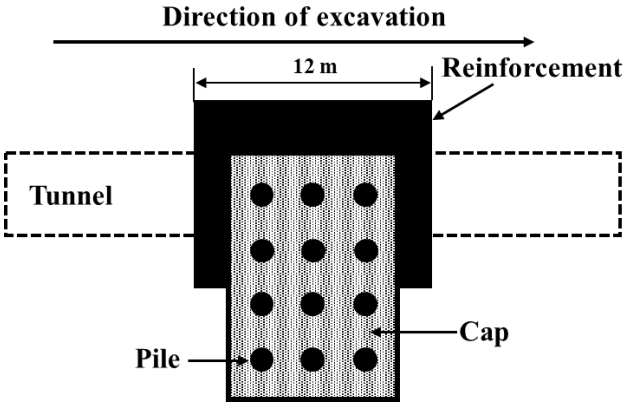

(c) Top view of analysis geometry

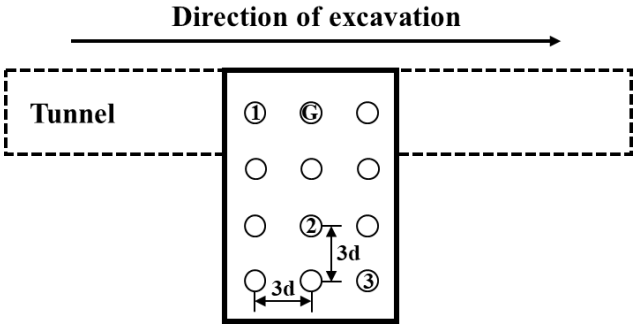

(d) Locations of piles in 4 × 3 pile group

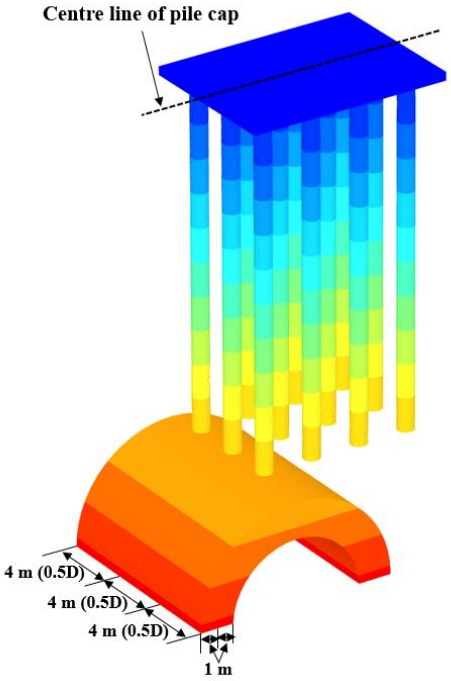

(e) Location of piles in 4 × 3 pile group (centre line of pile cap at $Y = 0$ m)

Fig. 2 Elements and geometries used in study analyses

Table 2 Summary of study pile locations and conditions

Study pile identifier	Ground reinforcement angle	Ground reinforcement thickness (T)	Pile location (shown in Fig. 2(d))	Remarks
DP-1	–	–	1	Design load condition
DP-2	–	–	2	
DP-3	–	–	3	
P-1	–	–	1	Pile group without ground reinforcement
P-2	–	–	2	
P-3	–	–	3	
RP1-1	180°	1 m	1	Pile group with ground reinforcement
RP1-2	180°	1 m	2	
RP1-3	180°	1 m	3	
RP2-1	180°	2 m	1	
RP2-2	180°	2 m	2	
RP2-3	180°	2 m	3	

Table 3 Material parameters assumed in the numerical modelling

Material	Model	γ_t (kN/m^3)	E' (MPa)	K_0	v'	c' (kPa)	φ' (°)
Soil (Lee 2012a)	Mohr–Coulomb	20	80	0.75	0.35	50	35
Grouted material	Mohr–Coulomb	25	800	0.01	0.2	250	35
Lining	Elastic	25	5,000 (s) 15,000 (h)	0.01	0.2	–	–
Pile/Pile cap		25	30,000	0.01	0.2	–	–

γ_t: unit weight of material; E': Young's modulus; K_0: lateral earth pressure coefficient at rest; v': Poisson's ratio; c': cohesion; φ': internal friction angle; s: soft shotcrete; h: hard shotcrete

conditions are given in Section 2.3. The pile cap was assumed to have a thickness(t) of 0.5 m. Table 1 summarises the five analyses carried out in the study. The analyses were conducted for the pile with the shortest separation distance from the tunnel (1), an inner pile (2), and the pile with the longest separation distance from the tunnel (3), as identified in Fig. 2(d). Table 2 presents the list of study piles identified according to pile location and reinforcement conditions. The groundwater level was not considered in this analysis.

2.2 Applied model and material properties

An elastic–plastic analysis was performed to simulate tunnel excavation. Boundary elements were applied to allow for slippage due to plastic yielding at the interface between the soil and the piles; this was done to analyse the shear stress transfer process at the interface between the soil and the piles. In addition, boundary elements were designated at the pile tip so that the pile tip and soil were separated when tensile force was generated on the pile. The volume loss was calculated by dividing the volume per unit width of lateral (X-direction) surface settlement at a specific point (Y/D = 0) in the tunnel excavation stage by the volume per unit width of the tunnel. Table 3 presents the properties of the materials and ground used in the numerical analysis, which are general material properties for weathered soil and concrete in South Korea (Lee 2012a).

For the properties of the grouting used in the reinforcement area, the method of Choi *et al.* (2003) for calculating the material properties of the grout body through inverse analysis was applied, and the elastic modulus and cohesion of the grouted section were increased to 10 and 5 times the original ground properties, respectively (under the assumption that the internal friction angle does not change).

The same property values applied to the piles were applied to the pile cap. For the weathered soil and grout body, an elastic–plastic model following the non-associated flow rule and Mohr–Coulomb's failure criterion were applied, and an isotropic elastic model was applied for the pile cap, piles, and lining. To consider the reduction in shear strength constants (c'_{int} for the pile surface–soil interface and φ'_{int} for the pile tip–soil interface) caused by pile construction, referring to the guidelines of Brinkgreve *et al.* (2015), we applied a strength reduction factor (R_{int}) of 0.7 and calculated the appropriate shear strength constants using the following equations

$$c'_{\text{int}} = R_{\text{int}} \times c'_{\text{soil}} \tag{1}$$

$$\tan\varphi'_{\text{int}} = R_{\text{int}} \times \tan\varphi'_{\text{soil}} \tag{2}$$

where c'_{soil} is the soil cohesion, φ'_{soil} is the internal friction

angle of the soil, and φ'_{int} is the interface friction angle (calculated as 26.1°).

2.3 Numerical analysis process

The numerical analysis did not include the change in ground stress caused by the effect of the embedment that occurs during pile construction; therefore, the piles were assumed to be cast in place. Tunnel excavation was performed between −5*D* and +5*D* (−40 m to +40 m) in the Y direction (Fig. 2(a)) over a total of 80 stages in increments of 1 m. Upon the completion of each stage of excavation, shotcrete lining was sprayed to a thickness of 200 mm on the excavated surface: it was applied in the form of soft shotcrete with an elastic modulus of 5,000 MPa, and in the following excavation stage, its material properties were converted to those of hard shotcrete with an elastic modulus of 15,000 MPa to simulate excavation. As shown in Fig. 2(e), grouting reinforcement was performed to ±0.75*D* (±6 m, for a total reinforcement of 12 m) in the Y direction from the pile cap centre line (Y = 0 m), and assuming that each reinforcement length was 0.5*D* (4 m), excavation was conducted in increments of 1 m after each reinforcement, for a total reinforcement of 12 m. (The steps flow as follows: reinforcement (4 m) → four excavations (1 m each) → reinforcement (4 m) → four excavations (1 m each) → reinforcement (4 m) → four excavations (1 m each).) The pile behaviour was analysed according to the following conditions for grouting reinforcement thickness: no reinforcement (P, T = 0 m), 1 m reinforcement thickness (RP1, T = 1 m), and 2 m reinforcement thickness (RP2, T = 2 m). The reinforcement angle in the X direction of the grouting was fixed at 180°. After reaching initial equilibrium, the design load (P_d) calculated through a separate analysis (PLT) was increased in stages (4,750 kN) and applied to the pile heads before tunnel excavation. To evaluate the analysis results, the axial pile force P_p at arbitrary depths was calculated using the formula $P_p = \sigma_{zz\_avg} \times A_s$, where σ_{zz_avg} is the averaged vertical stress value for a pile at a specified elevation, and A_s is the cross-sectional area of a pile. Shear stress at the interface between piles and soil was calculated by averaging the values for arbitrary depths.

3. Analysis results and evaluation

3.1 Determining the designed pile bearing capacity

Fig. 3 shows the load–settlement relationship of the piles calculated from a pile loading test simulation to determine the designed capacity of the piles. The relationship shown does not include tunnel excavation, and the compressive force on the pile head was increased in stages to simulate the loading test. As can be seen, there is an almost linear relationship between pile load and pile head settlement until the load on the pile head reaches approximately 7,500 kN; when load exceeding this value is applied, settlement suddenly occurs. This study also applied the method of Davisson (1972) to calculate the designed

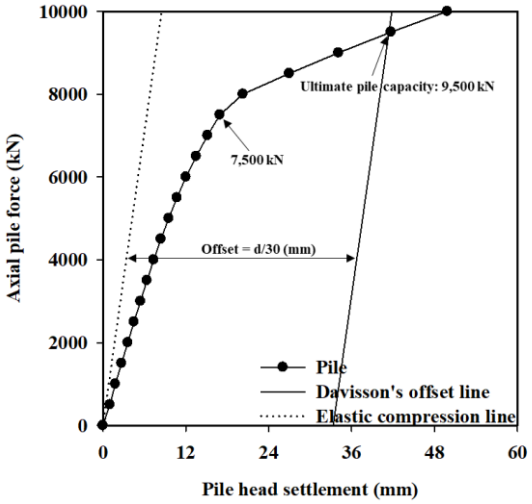

Fig. 3 Relationship between axial pile force and pile head settlement

capacity of the piles from the load–settlement relationship, by which the pile failure load was calculated as 9,500 kN. From this, the pile design load (P_d) was determined to be 4,750 kN by applying a safety factor (F_S) of 2.0 ((9,500 kN)/2 = 4,750 kN). Here, the settlement (Δ) of the pile head is 9.10 mm. To analyse the behaviour of piles already constructed, the design load (P_d) was applied to the pile head before tunnel excavation in three stages (1,583 kN → 3,166 kN → 4,750 kN). The behaviour of piles in use was simulated in this manner, after which staged tunnel excavation was performed.

3.2 Pile head settlement and soil surface settlement due to tunnel excavation

Fig. 4 shows the distributions of the normalised settlements by excavation stage, calculated using the analysis according to grouting reinforcement thickness in the pile group connected by the pile cap (Y/D is the normalised longitudinal extent). Δ_{gr} indicates the soil surface settlement caused by tunnel excavation at location G in the pile group under the Greenfield analysis conditions (in which there are no embedded piles and ground reinforcement is not considered), Δ_{p_net} indicates the tunnelling-induced pile head settlement, which excludes the pile settlement that developed under the application of the axial pile loading, and Δ_{gr_max} indicates the maximum soil surface settlement due to tunnel excavation under the Greenfield analysis conditions (Δ_{gr_max} = 8.9 mm). As shown in the figure, the normalised settlements $\Delta_{p\_net}/\Delta_{gr\_max}$ and $\Delta_{gr}/\Delta_{gr\_max}$ gradually increase as tunnel excavation progresses. The greatest soil surface and pile head settlement rates occurred as the tunnel excavation advanced through the points between Y/D = −1.5 and Y/D = +1.5, after which the rates of settlement due to excavation decreased substantially. Hence, pile settlement due to tunnel excavation occurs mainly in the range as tunnel excavation advances between points Y/D = −2.0 and Y/D = +2.0. For all

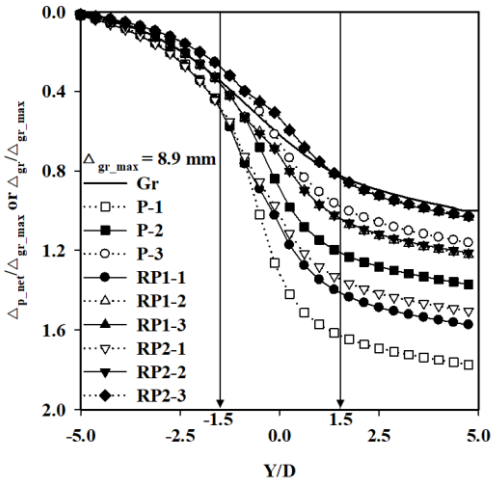

Fig. 4 Distributions of normalised pile head and soil surface settlements with normalised tunnel advancement Y/D (Δ_{gr_max} = 8.9 mm)

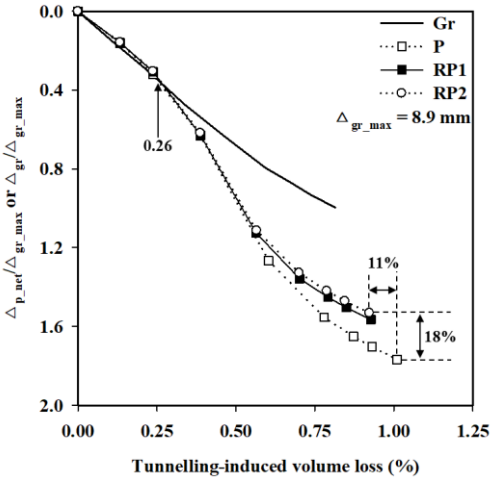

Fig. 5 Distributions of normalised tunnelling-induced pile head and Greenfield soil surface settlements with tunnelling-induced volume loss at Y/D = 0

piles, the final settlement of the pile head exceeded the final settlement of the soil surface under the Greenfield conditions; however, piles P-3, RP1-3, and RP2-3 showed less settlement than the soil surface under the Greenfield conditions before tunnel excavation passed near the part directly under the piles (Y/D = 0). This is because those piles are farthest from the tunnel and thus are less affected by soil settlement due to tunnel excavation. Pile RP2-1 showed approximately 15% less settlement than pile P-1 at the same location, for which ground reinforcement is not considered. Pile P-1, which is expected to be the most affected by soil settlement, showed approximately 70% greater pile head settlement than pile RP2-3, which is the least affected by soil settlement. In a pile group connected by a pile cap, pile head settlement varies with the location within the pile group, as exhibited by the differential settlement of the pile cap. Under condition P, the maximum pile cap settlement due to tunnel excavation was calculated as 16.7 mm, and the minimum as 9.7 mm, and under condition RP2, the maximum was 14.1 mm and the minimum was 8.9 mm. As settlement varied according to pile cap location, it is likely necessary to evaluate the serviceability of the structure according to differential settlement. Section 3.9 explains the evaluation of structural stability based on differential settlement in detail.

3.3 Pile head settlement and soil surface settlement according to volume loss

Fig. 5 shows the normalised tunnelling-induced pile head settlement ($\Delta_{p\_net}/\Delta_{gr\_max}$) and soil surface settlement under the Greenfield conditions ($\Delta_{gr}/\Delta_{gr\_max}$) according to the tunnelling-induced volume loss at location Y/D = 0. Here, $\Delta_{gr}/\Delta_{gr\_max}$ indicates settlement at location G in the pile group, and for $\Delta_{p\_net}/\Delta_{gr\_max}$, the settlement at location 1 of the pile group was calculated. As shown in the figure, the settlement of piles with and without reinforcement exhibited trends similar to that for soil surface settlement until the volume loss reached 0.26%, after which the pile settlement exceeded soil surface settlement as the volume loss increased. Lee (2013) reported a similar trend, in which the volume loss and pile settlement were larger than those under the Greenfield conditions if piles were present. Additionally, a similar trend was reported by Jacobsz (2002) from geotechnical centrifuge model tests. The volume loss and pile settlement were greatest under condition P; compared with the piles under condition RP2, volume loss and pile settlement were approximately 11% and 18% higher, respectively. This suggests that when the ground near the tunnel is not reinforced, both volume loss and pile settlement are higher than for the ground condition in which reinforcement is applied. Furthermore, few databases have been established for South Korea that consider volume loss either theoretically or practically, whereas for the UK, Macklin (1999) analysed and organised various volume losses for overconsolidated clay soils and reported volume losses within the range of approximately 0.5% to 3.0%. Accordingly, it is necessary in South Korea as well to perform construction management considering tunnelling-induced volume loss, prediction of settlement in nearby ground, and evaluations of structural stability.

3.4 Pile cap vertical settlement contour lines

Fig. 6 shows contour lines for vertical settlement of the pile cap according to reinforcement condition (no reinforcement, 1 m of grouting reinforcement, and 2 m of grouting reinforcement), calculated after tunnel excavation is complete. The figure presents a top view of the pile cap for each reinforcement condition to facilitate comparison between the conditions. Under condition P (no reinforcement), the area where pile cap settlement occurred was more widely distributed than under the other conditions. Moreover, under all conditions, settlement decreased as the distance from the tunnel to the pile cap

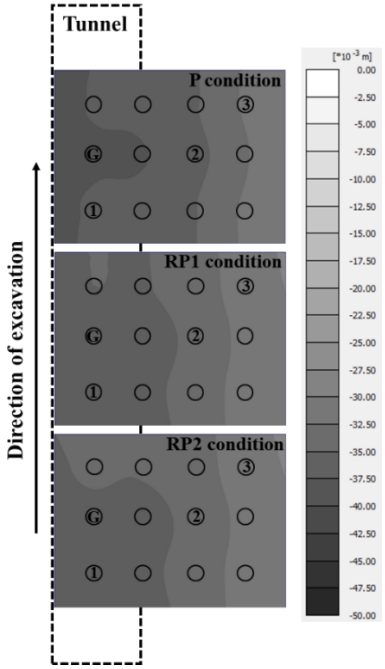

Fig. 6 Top view of vertical settlement of cap under three reinforcement conditions

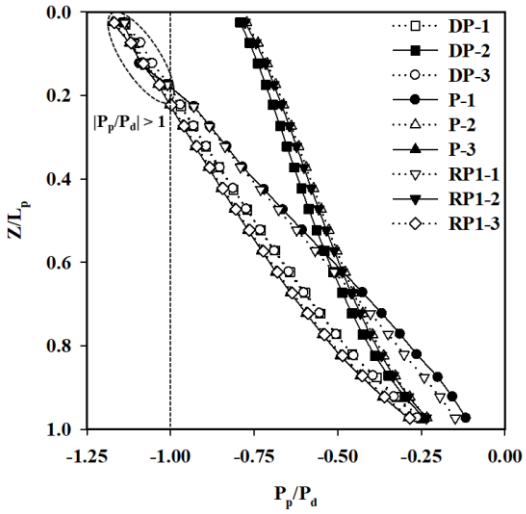

Fig. 7 Distributions of normalised axial pile forces with depth

increased, and settlement was greatest in the area of the pile cap directly above the tunnel, indicating that differential settlement occurred. The pile cap settlement amounts described in Section 3.2 are thus verified by contour lines.

3.5 Distribution of axial pile force

Fig. 7 shows distributions of normalised axial force (P_p/P_d) for the pile group according to reinforcement condition (no reinforcement and 1 m of grouting reinforcement), calculated with respect to the normalised pile depth (Z/L_p) after tunnel excavation is complete. (The axial force distributions under condition RP2, i.e., 2 m of grouting reinforcement, are omitted from the figure because they were nearly identical to those under condition RP1, i.e. 1 m of grouting reinforcement.) The figure also includes the axial force distribution of the design load applied to the pile heads before tunnel excavation. Here, P_p indicates the axial pile force at an arbitrary depth, and P_d indicates the design load (4,750 kN) applied to the pile head before tunnel excavation. As described earlier, the axial pile force was obtained by calculating the average vertical stress on the pile for an arbitrary depth and the axial pile force is expressed as an absolute value. Under the design load, the axial pile force gradually decreases as the depth increases; approximately 75% of the load is supported by surface friction, and only the remaining 25% is supported by the pile tip. Additionally, for piles 1 and 3, located on the outer edges of the pile group, P_p/P_d exceeded the design load near the pile head ($|P_p/P_d| > 1$); this is because the pile cap's weight is concentrated on the outer piles. In contrast, pile 2, located on the inside of the pile group, was less affected ($|P_p/P_d| < 1$). For pile 1, located closest to the tunnel, the proportion borne by skin friction on the pile increased to approximately 85% after tunnel excavation, and that borne by the tip decreased to approximately 15%. This indicates that even in a pile group connected by a pile cap and behaving as one unit, the piles located directly above the tunnel crown are more strongly affected by soil settlement. However, to closely investigate the distributions of the axial pile forces according to reinforcement condition, it is necessary to analyse the axial pile force induced purely by tunnelling, for which the influence of axial pile loading on the pile heads is removed.

To facilitate the clear identification of the changes in axial pile force due to tunnel excavation, Fig. 8 presents distributions of normalised tunnelling-induced axial pile force (P_n/P_d) according to reinforcement condition (no reinforcement, 1 m of grouting reinforcement, and 2 m of grouting reinforcement) with respect to the normalised pile depth (Z/L_p), where P_n indicates the axial pile force caused purely by tunnel excavation and the axial pile force is expressed as an absolute value. As shown in the figure, for pile 1, which is closest to the tunnel, the axial pile force due to tunnel excavation increases gradually from the soil surface to near $Z/L_p = 0.8$ and then decreases to the pile tip at $Z/L_p = 0.8$. Table 4 shows the normalised maximum compressive force ($P_{n\_(-)max}/P_d$) and maximum tensile force ($P_{n\_(+)max}/P_d$) acting on the piles according to analysis condition. For pile P-1, $P_{n\_(+)max}/P_d$ was +0.19, whereas RP1-1 and RP2-1 showed slightly lower values of approximately +0.15. Piles P-2 and RP1-2 exhibited an axial force distribution in the form of tensile force, whereas for pile RP2-2, which has the thickest reinforcement, the axial force distribution of compressive force was reversed. This is because the reinforcement effect is maximised as the reinforcement increases, and therefore soil settlement near the pile tip does not exceed the pile settlement. For piles P-3, RP1-3, and RP2-3, the piles farthest from the tunnel, the axial force distribution in the form of compressive force did not show a large difference from pile head to tip. Section 3.8 explains the mechanisms that generate tensile force and compressive force acting on the piles in detail.

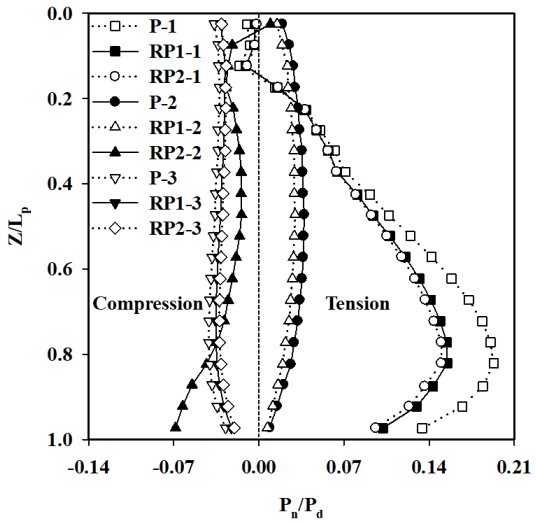

Fig. 8 Distributions of normalised tunnelling-induced axial pile forces with depth

Table 4 Computed maximum axial pile forces

Study pile	$P_{n\_(-)max}/P_d$	$P_{n\_(+)max}/P_d$
P-1	–	+0.19
RP1-1	–	+0.15
RP2-1	–	+0.15
P-2	–	+0.03
RP1-2	–	+0.02
RP2-2	−0.06	–
P-3	−0.04	–
RP1-3	−0.03	–
RP2-3	−0.03	–

$P_{n\_(-)max}/P_d$: normalised maximum compressive pile force; $P_{n\_(+)max}/P_d$: normalised maximum tensile pile force

3.6 Distribution of shear stress around piles

Fig. 9 shows the distributions of shear stress at the pile-adjacent soil interface calculated according to normalised pile depth (Z/L_p) after tunnel excavation is complete, for the condition of no reinforcement. The distributions of shear stress by design load before tunnel excavation and shear stress after tunnel excavation is complete are also shown. Here, the explanation of the shear stress is expressed as an absolute value. Piles DP-1 and DP-3, located on the outer edges of the pile group, exhibited trends in shear stress similar to those generated by the design load applied to the piles before tunnel excavation, whereas pile DP-2, located on the inside of the pile group, showed relatively low shear stress. Under the design load, shear stress decreased as pile depth increased from the pile head to near Z/L_p = 0.3, after which the shear stress increased again to the pile tip. In contrast, after tunnel excavation, unlike piles P-2 and P-3, pile P-1 showed a gradual decrease in shear stress as the pile depth increased, with a shear stress of approximately 50 kPa at the pile tip. This is because the relative

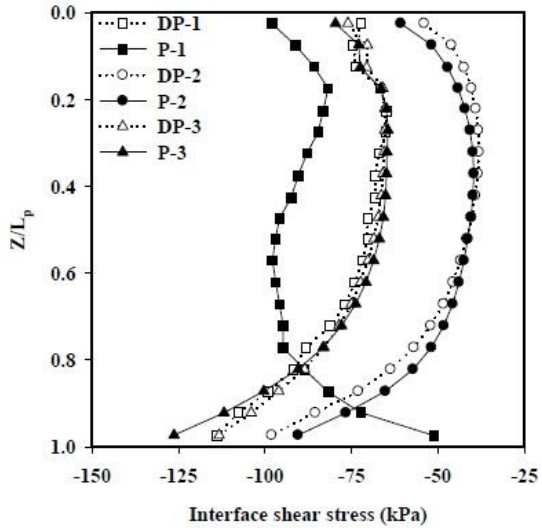

Fig. 9 Distributions of interface shear stress with depth (without reinforcement)

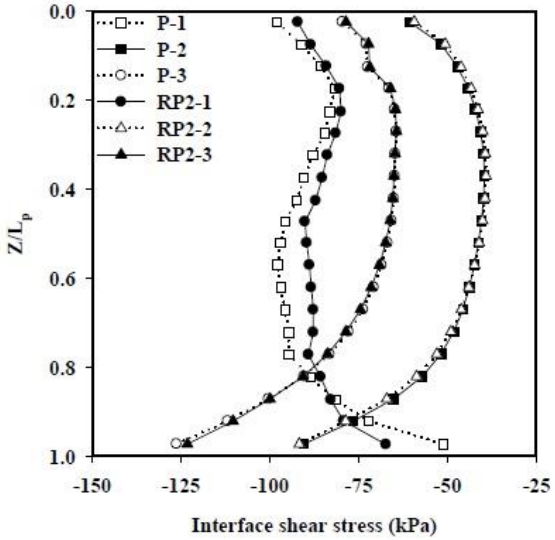

Fig. 10 Distributions of interface shear stress with depth (under two reinforcement conditions)

displacements at the pile-soil interface decrease; hence the shear stress near the pile tip reduces.

Fig. 10 shows the distributions of shear stress at the pile-adjacent soil interface according to reinforcement condition (no reinforcement and 2 m of grouting reinforcement) calculated with respect to the normalised pile depth (Z/L_p) after tunnel excavation is complete. To more clearly distinguish the differences in shear stress distributions according to reinforcement condition, Fig. 10 presents only the conditions of no reinforcement and 2 m grouting reinforcement; Fig. 11 presents detailed results including all reinforcement conditions for the distributions of shear stress induced purely by tunnelling. As shown in Fig. 10, the shear stress distributions displayed similar trends both without reinforcement and with 2 m of grouting reinforcement. Particularly for piles

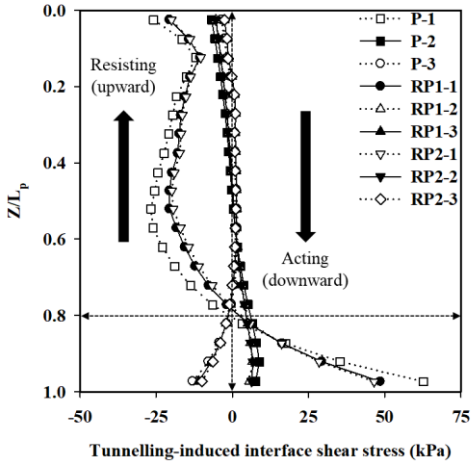

Fig. 11 Distributions of tunnelling-induced interface shear stress with depth

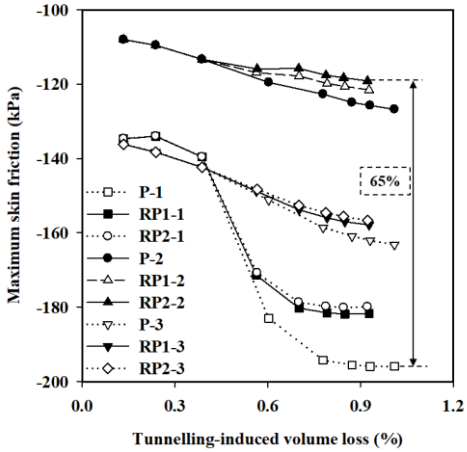

Fig. 12 Distributions of maximum skin friction on piles with tunnelling-induced volume loss at $Y/D = 0$

2 and 3, the shear stress distributions did not differ between the two conditions. Conversely, for pile 1, the shear stress values varied slightly, differing by approximately 16 kPa near the pile tip. This is because pile 1 is the pile closest to the tunnel and thus the one most affected by the reinforcement condition. However, to analyse the shear stress transfer mechanism in detail at the pile-soil interface associated with tunnel excavation according to reinforcement condition, the effect of the design load applied to the pile head should be excluded.

Fig. 11 shows the distributions of shear stress induced purely by tunnelling with respect to the normalised pile depth (Z/L_p) for piles 1-3 in the pile group under the three reinforcement conditions (no reinforcement and 1 m and 2 m grouting reinforcement). Here, the explanation of the shear stress is expressed as an absolute value. As shown in Fig. 11, pile 1 exhibited similar trends for all reinforcement conditions, whereas pile P-1 (with no reinforcement) showed relatively high shear stress compared with piles RP1-1 and RP2-1 at specific pile depths. Furthermore, for pile 1 under all reinforcement conditions, the sign of the shear stress value reversed near $Z/L_p = 0.8$, which signifies that the direction of shear force acting on the pile reversed at a particular depth (approximately $Z/L_p = 0.8$). In other words, from the pile head to a depth of $Z/L_p = 0.8$, pile settlement exceeded soil settlement and upward shear stress occurred, whereas from $Z/L_p = 0.8$ to the pile tip, soil settlement exceeded pile settlement and downward shear stress occurred. Hence, the pile showed an axial force distribution in the form of tensile force. Piles 2 and 3 showed similar trends for all reinforcement conditions, and for pile 2, the sign for shear stress changed near a depth of approximately $Z/L_p = 0.45$. This is similar to the above-described shear stress mechanism acting on pile 1, and therefore it is expected to show an axial force distribution in the form of tensile force. However, we can infer that the axial force will be low because of the small difference between the shear stress values near the pile head and those near the pile tip. Thus, the content explained in Section 3.5 is verified by the shear stress evaluation. Unlike that for piles 1 and 2, shear stress for pile 3 was upward from the pile head to near $Z/L_p = 0.2$, and shear stress was also upward from the pile tip to near $Z/L_p = 0.7$. In other words, upward shear stress occurred in two areas, the pile head and pile tip; the shear stress at the head was smaller than at the tip, causing an axial stress distribution in the form of compressive force on the pile. Section 3.8 further explains the direction of shear stresses.

3.7 Maximum skin friction on piles according to volume loss

Fig. 12 shows the maximum friction acting on the piles according to tunnelling-induced volume loss at location $Y/D = 0$ under the three reinforcement conditions (no reinforcement and 1 m and 2 m grouting reinforcement) at piles 1-3 in the pile group. Here, the values of tunnelling-induced volume loss do not start from zero because these are to determine the maximum skin friction acting for the specific separation distance from the centre line of pile cap. As shown in the figure, the maximum friction acting on a pile varies with its location within the pile group, and the maximum friction increases as the volume loss increases. Pile 2 in the pile group showed a smaller maximum friction than the other piles; this is because, owing to the group effect acting on the pile group, the piles and adjacent soil settle together in the form of a block, causing very small relative shear displacement (Lee 2012c). Additionally, the maximum skin friction acting on pile P-1 was approximately 65% larger than that on pile RP2-2, which is located on the inside of the pile group and has the thickest reinforcement. Because the piles differ in their behaviour according to their location, the reinforcement conditions, and the extent of tunnel excavation, a further research is obviously needed that considers these influencing factors.

3.8 Distribution of relative pile displacement

Fig. 13 shows the normalised distributions of relative

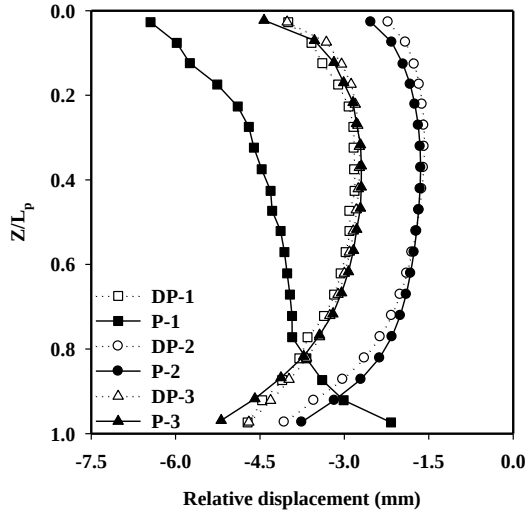

Fig. 13 Distributions of relative pile displacements with depth

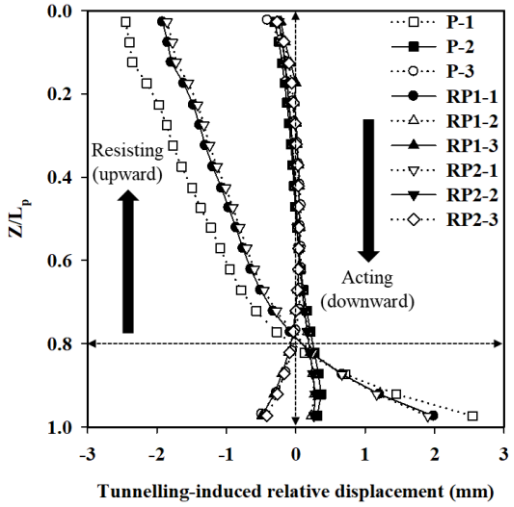

Fig. 14 Distributions of tunnelling-induced relative pile displacements at the pile–soil interface with depth

displacements at the interface between the piles and soil calculated with respect to pile depth (Z/L_p) for piles 1-3 and 3 in the pile group under the condition of no reinforcement after tunnel excavation is complete. Here, the relative displacement is expressed as an absolute value. Because of the design load applied to the pile head and pile cap before tunnel excavation, the pile settlement exceeds soil settlement for all sections of the pile. The distributions of relative pile displacements under the design load exhibited similar trends for piles DP-1 and DP-3, which are located on the outer edges of the pile group, whereas pile DP-2, located on the inside of the pile group, showed a smaller relative displacement. Pile P-1 showed the largest relative displacement occurring for the piles after tunnel excavation without reinforcement, and the remaining piles (P-2 and P-3) showed relative displacements similar to those under the design load before tunnel excavation. Furthermore, after tunnel excavation, the relative displacement of pile P-1 gradually decreased as the depth increased from the pile head and was approximately 2.0 mm in magnitude at the pile tip. In contrast, for the piles under the other conditions, the relative displacement decreased as the pile depth increased and then increased again after a certain point. As the changes in relative displacement vary with the pile's location within the pile group, it is necessary to evaluate the relative displacement induced purely by tunnelling.

Fig. 14 shows the relative pile displacements induced purely by tunnelling with respect to the normalised pile depth (Z/L_p) for piles 1-3 in the pile group under the three reinforcement conditions (no reinforcement and 1 m and 2 m grouting reinforcement). Pile 1 showed a larger relative displacement than the other two piles for all reinforcement conditions; it was largest for pile P-1, which had no reinforcement. For pile 1, the sign of the relative displacement value reversed near $Z/L_p = 0.8$, which signifies that the direction of relative displacement acting on the pile is reversed at a specific depth (approximately $Z/L_p = 0.8$). Thus, from $Z/L_p = 0.8$ to the pile tip, downward friction due to tunnelling-induced soil settlement acts on the pile, whereas from the pile head to $Z/L_p = 0.8$, upward frictional resistance occurs, in which the soil resists pile settlement. Additionally, pile 2 exhibited a relative displacement mechanism similar to that of pile 1; however, because of the small difference in relative displacements of the inner piles, the frictional resistance was not large, leading to small shear stress. Hence, the shear stress distribution described above is verified by the tunnelling-induced relative displacement. At the tip of pile 3, unlike piles 1 and 2, negative relative displacement occurs and results in upward frictional resistance, and as there is almost no relative displacement at the upper part of the pile, there is nearly no frictional resistance, thus the compressive pile force on the pile was obtained.

3.9 Stability evaluation through analysis of pile cap behaviour

Fig. 15 is a plot showing the building damage criterion proposed by Son and Cording (2005) based on the relationship between angular distortion and lateral strain in the structure. Using this, we evaluated the stability of the pile cap for the three reinforcement conditions (no reinforcement and 1 m and 2 m grouting reinforcement). As the average lateral strain in the pile cap was approximately 2×10^{-4} and the average angular distortion was approximately 4×10^{-4} for all reinforcement conditions, the values are concentrated near the origin of the damage plot in Fig. 15. The stability evaluation indicates that the level of damage is 'negligible'. The structure simulated in the numerical analysis comprised 12 large-diameter piles, each having a diameter of 1 m, and because the pile heads are all connected to a pile cap, the structure's stability during tunnel excavation activity is maximised. Moreover, Lee *et al.* (2012) conducted a numerical analysis and evaluated the stability of a structure based on the structure damage diagram proposed by Burland (1995) and reported a level of stability indicating that damage to the structure due to

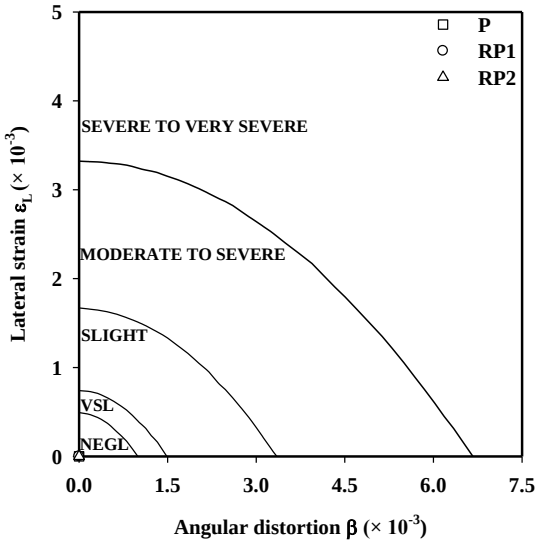

Fig. 15 Structure damage evaluation criterion based on angular distortion (β) and lateral strain (ε_L) (Son and Cording 2005)

tunnel excavation would be 'negligible.' This is similar to the findings of the present study. That is, although pile settlement does occur because of tunnelling-induced soil settlement, this is unlikely to adversely affect the superstructure in the case of a pile group because the piles are bound together by the pile cap. However, problems may arise in the superstructure if the face pressure is small, as in shield TBM construction performed in soft soil or weak rock. In addition, Finno *et al.* (2005) reported that it is not ideal to perform all stability evaluations for diverse structures by using damage diagrams. Specifically, they reported that the evaluation methods do not adequately account for the structural properties, or account for the deformation pattern caused the excavation-induced ground movements at buildings. Therefore, future research must evaluate the serviceability of superstructures under tunnel excavation conditions with consideration of the various governing factors such as characteristics of superstructures, tunnelling methods and ground conditions.

4. Conclusions

In this study, a three-dimensional finite element analysis was performed to examine the behaviour of piles, connected by a pile cap, when a tunnel passes underneath a pile group. Based on the results, we analysed the tunnelling-induced pile settlement, axial force, shear stress, and relative displacement and evaluated structural stability by analysing pile cap behaviour. The following points list the main findings and the conclusions that were drawn.

1. In the tunnel excavation stage, the largest soil surface and pile head settlement rates occurred when the tunnel excavation passed through the points from $Y/D = -1.5$ to $Y/D = +1.5$, after which the rates of settlement due to tunnel excavation decreased substantially. RP2-1 showed approximately 15% less settlement than the piles under condition P(P: without ground reinforcement, RP: with ground reinforcement). Moreover, the volume loss and pile settlement were greatest under condition P; compared with pile 1 under condition RP2, volume loss and pile settlement were approximately 11% and 18% higher, respectively. This indicates that when reinforcement is considered, both the volume loss and pile settlement increase over those in the condition in which reinforcement is not considered.
2. Under the design load (pile loading), the axial pile force gradually decreased as the depth increased; approximately 75% of the load was supported by surface friction, and only the remaining 25% was supported by the pile tip. By contrast, for pile 1, located closest to the tunnel, the proportion borne by skin friction on the pile increased to approximately 85% after tunnel excavation, and that borne by the tip decreased to approximately 15%. This indicates that even in a pile group connected by a pile cap and behaving as one unit, the piles located directly above the tunnel crown are more strongly affected by soil settlement. Moreover, piles P-2 and RP1-2 exhibited an axial force distribution in the form of tensile force, whereas for pile RP2-2, the axial force distribution of compressive force was reversed. This is because the reinforcement effect is maximised as the reinforcement increases, and therefore soil settlement near the pile tip does not exceed the pile settlement.
3. Pile P-1, under the no-reinforcement condition, showed a shear stress value greater than that of piles RP1-1 and RP2-1 at the same pile depths. Furthermore, for pile 1 under all reinforcement conditions, the sign of the shear stress value reversed near $Z/L_p = 0.8$, which signifies that the direction of shear force is reversed. Unlike that for piles 1 and 2, shear stress for pile 3 was upward at the pile head and pile tip; the shear stress value at the head was smaller than at the tip, causing an axial stress distribution in the form of compressive force on the pile.
4. The relative displacement of pile 1 was greater than that of the other piles under all reinforcement conditions, and pile P-1 showed the largest relative displacement. For pile 1, the sign of the relative displacement value reversed near $Z/L_p = 0.8$, which signifies that the direction of displacement acting on the pile is reversed at a specific depth. In other words, downward friction acts on the section of the pile within a specific range of depths, whereas upward frictional resistance, in which the soil resists pile settlement, acts on other specific sections.
5. The measurements of lateral strain and angular distortion of the pile cap found that under all reinforcement conditions, these were concentrated at the origin of the damage plot, which corresponds to 'negligible' damage in the stability evaluation. Although pile settlement occurs that is due to tunnelling-induced soil settlement, this is unlikely to adversely affect the superstructure in the case of a pile group because the piles are bound together by the pile cap. However, tunnel excavation in ultra-soft soil can lead to problems in the superstructure, and therefore research on the serviceability and stability of superstructure according to tunnel excavation conditions must consider the various influencing factors.

Acknowledgements

This research was supported by a grant (2019-MOIS33-005) of Lower-level and Core Disaster-Safety 329 Technology Development Program funded by the Ministry of Interior and Safety (MOIS, Korea) and this research was supported by Basic Science Research Program through the National Research Foundation of Korea(NRF) funded by the Ministry of Education(2017R1D1A1B05035579, 2022R1A6A3A01085973).

References

Ayasrah, M., Qiu, H., Zhang, X. and Daddow, M. (2020), "Prediction of ground settlement induced by slurry shield tunnelling in granular soils", *Civil Eng. J.*, **6**(12), 2273-2289. https://doi.org/10.28991/cej-2020-03091617.

Ayasrah, M., Qiu, H. and Zhang, X. (2021), "Influence of cairo metro tunnel excavation on pile deep foundation of the adjacent underground structures: Numerical study", *Symmetry*, **13**(3), 426. https://doi.org/10.3390/sym13030426.

Boscardin, M.D. and Cording, E.J. (1989), "Building response to excavation-induced settlement", *J. Geotech. Eng. ASCE*, **115**(1), 1-21. https://doi.org/10.1061/(ASCE)0733-9410(1989)115:1(1).

Burland, J.B., Broms, B.B. and de Mello, V.F.B. (1977), "Behavior of foundations and structures", *Proceedings of the 9th International Conference on Soil Mechanics and Foundation Engineering*, Japanese Geotechnical Society, Tokyo, Japan.

Burland, J.B. (1995), "Assessment of risk of damage to buildings due to tunnelling and excavations", *Proceedings of the 1st International Conference on Earthquake Geotechnical Engineering*, IS-Tokyo.

Brinkgreve, R.B.J., Kumarswamy, S. and Swolfs, W.M. (2015), "Reference manual", *Plaxis 3D 2015 user's manual*, Delft, 1-284.

Cheng, C.Y., Dasari, G.R., Chow, Y.K. and Leung, C.F. (2007), "Finite element analysis of tunnel-soil-pile interaction using displacement controlled model", *Tunn. Undergr. Sp. Tech.*, **22**(4), 450-466. https://doi.org/10.1016/j.tust.2006.08.002.

Choi, Y.G., Park, J.H., Woo, S.B. and Jeong, Y.J. (2003), "Reinforcing effect of FRP multi-step grouting for NATM tunnel through weathered zone", *KSCE 2003 convention program*, Seoul, Korea.

Choi, H.J., Kim, S.G., Jang, K.J., Shim, J.D. and Eun, S.J. (2005), "Case Study on Tunnel Design under Terminal Structure of Gimpo Airport", *Proceedings of the KSCE Tunnel Committee Special Conference*, Seoul, Korea.

Davisson, M.T. (1972), "High capacity piles", *Proceedings of Lecture Series in Innovations in Foundation Construction*, ASCE, Illinois Section.

Dias, T.G.S. and Bezuijen, A. (2014a), "Pile tunnel interaction: Literature review and data analysis", *Proceedings of the ITA World Tunnel Congress 2014*, Iguassu Falls, Brazil, May.

Dias, T.G.S. and Bezuijen, A. (2014b), "Pile-tunnel interaction: A conceptual analysis", *Proceedings of the 8th International Symposium on Geotechnical Aspects of Underground Construction in Soft Ground*, CRC Press, Seoul, Korea, August.

Finno, R.J., Voss, F.T., Rossow, E. and Blackburn, J.T. (2005), "Evaluating damage potential in buildings affected by excavations", *J. Geotech. Geoenviron. Eng. ASCE*, **131**(10), 1199-1210. https://doi.org/10.1061/(ASCE)1090-0241(2005)131:10(1199).

Hartono, E., Leung, C.F., Shen, R.F., Chow, Y.K., Ng, Y.S., Tan, H.T. and Hua, C.J. (2014), "Behaviour of pile above tunnel in clay", *Proceedings of the 8th International Conference on Physical Modelling in Geotechnics*, Perth, Australia, January.

Hong, Y., Soomro, M.A. and Ng, C.W.W. (2015), "Settlement and load transfer mechanism of pile group due to side-by-side twin tunnelling", *Comput. Geotech.*, **64**, 105-119. https://doi.org/10.1016/j.compgeo.2014.10.007.

Jacobsz, S.W. (2002), "The effects of tunnelling on piled foundations", Ph.D. Thesis, University of Cambridge, Cambridge, U.K.

Jue, K.S. and Na, D.S. (2005). "A study on the construction of tunnel near the piles of foundation of an overpass", *Proceedings of the KSCE Tunnel Committee Special Conference*.

Jeon, Y.J. and Lee, C.J. (2015), "A study on the behaviour of single piles to adjacent tunnelling in stiff clay", *J. Korean Geo-Environ. Soc.*, **16**(6), 13-22. https://doi.org/10.14481/jkges.2015.16.6.13.

Jeon, Y.J., Kim, S.H. and Lee, C.J. (2015), "A study on the effect of tunnelling to adjacent single piles and pile groups considering the transverse distance of pile tips from the tunnel", *J. Korean Tunnelling and Underground Space Association*, **17**(6), 637-652. https://doi.org/10.9711/KTAJ.2015.17.6.00

Jeon, Y.J., Kim, S.H., Kim, J.S. and Lee, C.J. (2017), "A study on the effects of ground reinforcement on the behaviour of pre-existing piles affected by adjacent tunnelling", *J. Korean Tunnelling and Underground Space Association*, **19**(3), 389-407. https://doi.org/10.9711/KTAJ.2017.19.3.389.

Jeon, Y.J., Kim, J.S., Jeon, S.C., Jeon, S.J., Park, B.S. and Lee, C.J. (2018), "A study on the behaviour of single piles to adjacent Shield TBM tunnelling by considering face pressures", *J. Korean Tunnelling and Underground Space Association*, **20**(6), 1003-1022. https://doi.org/10.9711/KTAJ.2018.20.6.1003.

Jeon, Y.J., Jeon, S.C., Jeon, S.J. and Lee, C.J. (2020a), "Study on the behaviour of pre-existing single piles to adjacent shield tunnelling by considering the changes in the tunnel face pressures and the locations of the pile tips", *Geomech. Eng.*, **21**(2), 187-200. https://doi.org/10.12989/gae.2020.21.2.187.

Jeon, Y.J., Jeon, S.C., Jeon, S.J. and Lee, C.J. (2020b), "A study on the behaviour of pre-existing single piles to adjacent shield TBM tunnelling from three-dimensional finite element analyses", *J. Korean Tunnelling and Underground Space Association*, **22**(1), 23-46. https://doi.org/10.9711/KTAJ.2020.22.1.023.

Lee, C.J. and Chiang, K.H. (2007), "Responses of single piles to tunnelling-induced soil movements in sandy ground", *Canadian Geotechnical Journal*, **44**(10), 1224-1241. https://doi.org/10.1139/T07-050

Lee, C.J. (2012a), "Three-dimensional numerical analyses of the response of a single pile and pile groups to tunnelling in weak weathered rock", *Tunn. Undergr. Sp. Tech.*, **32**, 132-142. https://doi.org/10.1016/j.tust.2012.06.005.

Lee, C.J. (2012b), "Behaviour of single piles and pile groups in service to adjacent tunnelling conducted in the lateral direction of the piles", *J. Korean Tunnelling and Underground Space Association*, **14**(4), 337-356.

Lee, C.J. (2012c), "The response of a single pile and pile groups to tunnelling performed in weathered rock", *J. Korean Society of Civil Engineers*, **32**(5), 199-210.

Lee, S.W., Choy, C.K.M. and Tse, S.C. (2012), "3D Numerical modelling of tunnelling intersecting piles", *Geotechnical Aspects of Underground Construction in Soft Ground*, 919-925.

Lee, C.J. (2013), "Numerical analysis of pile response to open face tunnelling in stiff clay", *Comput. Geotech.*, **51**, 116-127. https://doi.org/10.1016/j.compgeo.2013.02.007.

Lee, C.J. and Jeon, Y.J. (2015), "A study on the effect of the locations of pile tips on the behaviour of piles to adjacent tunnelling", *J. Korean Tunnelling and Underground Space Association*, **17**(2), 91-105.

https://doi.org/10.9711/KTAJ.2015.17.2.091.
Lee, C.J., Jeon, Y.J., Kim, S.H. and Park, I.J., (2016), "The influence of tunnelling on the behaviour of pre-existing piled foundations in weathered soil", *Geomech. Eng.*, **11**(4), 553-570. https://doi.org/10.12989/gae.2016.11.4.553.
Lee, Y.J. (2008), "A boundary line between shear strain formations associated with tunneling adjacent to an existing piled foundation", *J. Korean Tunnelling and Underground Space Association*, **10**(3), 283-293.
Liu, C., Zhang, Z. and Regueiro, R.A. (2014), "Pile and pile group response to tunnelling using a large diameter slurry shield - Case study in Shanghai", *Comput Geotech.*, **59**, 21-43. https://doi.org/10.1016/j.compgeo.2014.03.006.
Macklin, S.R. (1999), "The prediction of volume loss due to tunnelling in overconsolidated clay based on heading geometry and stability number", *Ground Eng.*, **32**(4), 30-33.
Marshall, A.M. (2009), "Tunnelling in sand and its effect on pipelines and piles", Ph.D. Thesis, University of Cambridge, Cambridge, U.K.
Mair, R.J. and Williamson, M.G. (2014), "The influence of tunnelling and deep excavation on piled foundations", *Geotechnical Aspects of Underground Construction in Soft Ground*, Seoul, Korea, August.
Ng, C.W.W., Lu, H. and Peng, S.Y. (2013), "Three-dimensional centrifuge modelling of the effects of twin tunnelling on an existing pile", *Tunn. Undergr. Sp. Tech.*, **35**, 189-199. https://doi.org/10.1016/j.tust.2012.07.008.
Ng, C.W.W. and Lu, H. (2014), "Effects of the construction sequence of twin tunnels at different depths on an existing pile", *Can. Geotech. J.*, **51**(2), 173-183. https://doi.org/10.1139/cgj-2012-0452.
Ng, C.W.W., Soomro, M.A. and Hong, Y. (2014), "Three-dimensional centrifuge modelling of pile group responses to side-by-side twin tunnelling", *Tunn. Undergr. Sp. Tech.*, **43**, 350-361. https://doi.org/10.1016/j.tust.2014.05.002.
Pang, C.H. (2006), "The effects of tunnel construction on nearby pile foundation", Ph.D. Thesis, The National University of Singapore, Singapore.
Plaxis 3D (2020), *Reference Manual, in Plaxis 3D User's Manual.*
Qiu, H., Wang, Z., Ayasrah, M., Fu, C. and Gang, L. (2022), "Numerical study on the reinforcement measures of tunneling on adjacent piles", *Symmetry*, **14**(2), 288. https://doi.org/10.3390/sym14020288.
Selemetas, D. (2005), "The response of full-scale piles and piled structures to tunnelling", Ph.D. Thesis, University of Cambridge, U.K.
Selemetas, D. and Standing, J.R. (2017). "Response of full-scale piles to EPBM tunnelling in London Clay", *Géotechnique*, **67**(9), 823-836. https://doi.org/10.1680/jgeot.SIP17.P.126.
Son, M. and Cording, E.J. (2005). "Estimation of building damage due to excavation-induced ground movements", *J. Geotech. Geoenviron. Eng. ASCE*, **131**(2), 162-177. https://doi.org/10.1061/(ASCE)1090-0241(2005)131:2(162).
Soomro, M.A., Ng, C.W.W., Memon, N.A. and Bhanbhro, R. (2018), "Lateral behaviour of a pile group due to side-by-side twin tunnelling in dry sand: 3D centrifuge tests and numerical modelling", *Comput. Geotech.*, **101**, 48-64. https://doi.org/10.1016/j.compgeo.2018.04.010.
Williamson, M.G. (2014), "Tunnelling effects on bored piles in clay", Ph.D. Thesis, University of Cambridge, Cambridge, U.K.